JACS
JOURNAL OF THE AMERICAN CHEMICAL SOCIETY

Communication

pubs.acs.org/JACS

Nanocrystals of a Metal–Organic Complex Exhibit Remarkably High Conductivity that Increases in a Single-Crystal-to-Single-Crystal Transformation

Kristin M. Hutchins,[†] Thilini P. Rupasinghe,[†] Lindsay R. Ditzler,[†] Dale C. Swenson,[†] John R. G. Sander,[†] Jonas Baltrusaitis,[‡] Alexei V. Tivanski,*[,†] and Leonard R. MacGillivray*[,†]

[†]Department of Chemistry, University of Iowa, Iowa City, Iowa 52242-1294 United States

[‡]PhotoCatalytic Synthesis Group, University of Twente, 7522 NB Enschede, The Netherlands

Supporting Information

ABSTRACT: Ag(I) is used to form a π-stacked metal–organic solid that exhibits remarkably high electrical conductivity. The solid undergoes a single-crystal-to-single-crystal [2+2] photodimerization to generate a 1D coordination polymer with over 40% higher conductivity. The Ag(I) complex represents the first example of an increase in conductivity resulting from a [2+2] photodimerization. Density of states calculations show a higher contribution from Ag(I) ions to the valence band in the photodimerized solid, supporting the increase in conductivity.

Crystal engineering is under increasing development,[1] with emerging applications in areas such as reactivity,[2] porosity,[3] and magnetism.[4] In this context, the design of organic semiconductor materials using principles of crystal engineering remains in early stages.[5] Applications of organic semiconductors include flexible electronics, smart cards, and solar panels among others.[6] A current challenge lies in achieving face-to-face π-stacking of candidate semiconductor molecules. Crystal engineering offers an opportunity to design semiconductor materials with structurally and electrically favorable arrangements of molecules.[7] The relevance of extending crystal engineering to nanoscale electronics is also important since electronic materials of nanoscale dimensions are promising to fabricate solar cells[8] and optoelectronic devices.[9] Nanocrystalline materials can also uniquely offer long-range order, well-defined molecular packing, and fewer structural defects, making such materials desirable to understand intrinsic electronic behavior.[10,11]

Whereas purely organic π-rich molecules (e.g., pentacene) have been pursued as building blocks of semiconductor materials, the integration of metal atoms into materials with favorable electrical conductivity is at a nascent stage.[7,12] The directionality of coordination bonds supported by transition metal ions can be exploited to achieve face-to-face stacking[13] that leads to favorable enhancement of conductivity.[14,15] In this context, a transition metal–organic complex of relatively high conductivity is $[Ag_2([1,10]phenanthrolin\text{-}2\text{-}one)_2]$. The solid consists of chelated Ag(I) ions that stack face-to-face and afford a solid with a conductivity of 14 S·cm^{-1}.[7]

A major tenet of crystal engineering is that supramolecular synthons provide means to achieve and tune properties of molecular solids. For solids based on Ag(I) ions, Ag···Ag interactions and Ag–N(pyridyl) bonds[16] are ubiquitous in the crystal engineering of metal–organic materials yet have remained unexplored to control properties of semiconductor materials. The synthons have, however, been employed to enforce π-stacking of olefins that undergo single-crystal-to-single-crystal (SCSC) [2+2] photodimerizations, which suggests opportunities to develop solids with both enhanced conductivity and reactivity.[17,18] Such solids would be attractive as components for photoactivated molecular switches,[19] 3D data storage,[20] and nanoscale photomechanical actuators.[21,22]

Here, we report the Ag-based metal–organic solid $[Ag_2(4\text{-stilbz})_4][CF_3SO_3]_2$ (**1**) that exhibits remarkably high electrical conductivity of 20.8 ± 1.3 S·cm^{-1} (Scheme 1). The solid is sustained by Ag···N(pyridine) bonds that organize 4-stilbz into a face-to-face π-stacked geometry. The olefin undergoes a SCSC [2+2] photodimerization to give $[Ag_2(4\text{-pyr-ph-cb})_2][CF_3SO_3]_2$ (**2**) that results in over a 40% increase in electrical conductivity to 37.0 ± 4.1 S·cm^{-1} as determined by conductive probe atomic force microscopy (CP-AFM). The SCSC reaction generates a 1D coordination

Scheme 1. Conductivity of Nanocrystals of Ag(I) Complex Using AFM (Anions Omitted for Clarity)

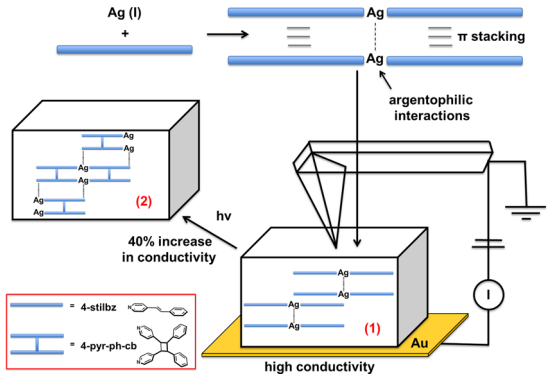

Received: December 27, 2013
Published: April 23, 2014

   dx.doi.org/10.1021/ja4131774 | J. Am. Chem. Soc. 2014, 136, 6778–6781

polymer accompanied by the formation of Ag···C(phenyl) forces and a blue shift in fluorescence. Density of states (DOS) calculations support the origin of increase in conductivity to be ascribed to increased contribution of the Ag(I) metal ions at the top edge of the valence band in **2** relative to **1**. To our knowledge, an increase in conductivity of a solid that results from a [2+2] photodimerization has not been reported. We also demonstrate comparable effects in isostructural $[Ag_2(4\text{-stilbz})_4][CO_2CF_3]_2$ (**3**) that generates SCSC photoproduct $[Ag_2(4\text{-pyr-ph-cb})_2][CO_2CF_3]_2$ (**4**).[23]

The focus of our study is dinuclear **1**, which is isostructural with **3**.[23] Single crystals of **1** were grown via slow evaporation of a 2:1 molar solution of 4-stilbz and $AgCF_3SO_3$ in acetonitrile. The formation of **1** was confirmed using powder and single-crystal X-ray diffraction (XRD).[24] The components are sustained by a combination of argentophilic forces (Ag(1)···Ag(1) distance = 3.50 Å) and Ag−N(pyridine) bonds (N(1) 2.153(5), N(2) 2.144(5) Å) (Figure 1). The carbon−carbon

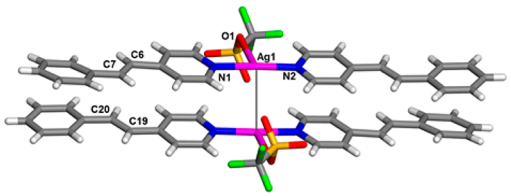

Figure 1. X-ray crystal structure of **1**. Interatomic distances (Å): C(6)···C(19) 3.80, C(6)···C(20) 3.85, C(7)···C(19) 4.09, C(7)···C(20) 4.27. Highest occupancies for disordered anions.

double bonds lie criss-crossed and separated by 3.90 Å. With the exception of the nature of the coordinating anions (Ag(1)−O(1) 2.63(7) Å), metrics related to packing of **1** make it virtually identical to **3** (including disorder of the anion).[23] The isostructural packing is defined by 1D quadruple face-to-face π-stacked arrays. The olefin of **1**, in contrast to **3**, however, lacks disorder. The anions lie orthogonal to the olefins, with the $-CF_3$ group pointing away from the metal and in a plane parallel to the pyridyl moieties.

The geometry of the stacked olefins of **1** is suitable for a solid-state [2+2] photodimerization.[25] Thus, single crystals and powdered crystalline samples of **1** were thus exposed to broadband UV irradiation for a period of 30 h.[23] Visual inspection of the single crystals demonstrated the morphologies and transparent appearance to be retained upon exposure to UV radiation. ^{1}H NMR spectroscopy showed the disappearance of 4-stilbz and formation of 4-pyr-ph-cb stereoselectively and in 100% yield (see SI, Figure S6). The photodimerization likely involved pedal motion of the C═C units.[26,27] Moreover, a single-crystal X-ray analysis[28] confirmed the reaction of **1** to occur via a SCSC transformation to give **2**. In the solid, the resulting cyclobutane ligand lies disordered such that 4-pyr-ph-cb occupies two orientations [occupancies: 0.538(9) and 0.462(9)] and the anion is also heavily disordered. Similar to the SCSC reaction of **3** to **4**,[23] the photoreaction was accompanied by repositioning of the Ag(I) ions (Ag···Ag = 5.05 Å), rotation of the counter triflate anions, and generation of Ag···C(phenyl) forces (Ag(1)···C(50) = 2.79 Å, Ag(2)···C(11) = 2.75 Å) (Figure 2) to give a 1D coordination polymer.

We next measured the electrical conductivity of **1**. Initial experiments were performed on single crystals of millimeter dimensions and plate morphologies using a two-point probe technique.[7] All attempts to measure current resulted in no

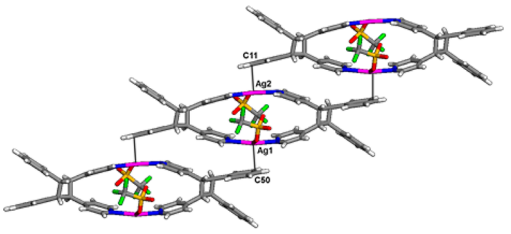

Figure 2. Ag···C(phenyl) forces and 1D coordination polymer upon SCSC photodimerization of **1** to **2**. Highest occupancies for disordered atoms.

measurable response, with the crystals repeatedly cleaving. We ascribe the inability to detect current to the crystals being extremely fragile, which likely results in an accumulation of cleavage planes that disrupt and shear the 1D stacked arrays.[23]

Given the fragility of the millimeter-sized crystals, we examined nanometer-sized crystals of **1** using CP-AFM. The technique has been used to characterize electrical properties of organic crystals and polymers.[29−32] The method allows measurements of conductivities on multi-nanometer length scales, which are considered indicative of intrinsic conductivity of a solid.[18,33]

To form nanocrystals of **1**, we employed sonochemistry. That sonochemistry affords crystals of nanoscale dimensions has been realized in inorganic-based solids[34] and organic co-crystals.[35] Thus, 4-stilbz and $AgCF_3SO_3$ were separately dissolved in minimal ethanol and simultaneously injected into hexanes under ultrasonic irradiation for a period of 2 min.[35,36] Powder X-ray diffraction (PXRD) confirmed the resulting white precipitate as **1** (see SI, Figure S1). AFM imaging revealed nanosized crystals that ranged from 30 to 200 nm (Figure 3a).

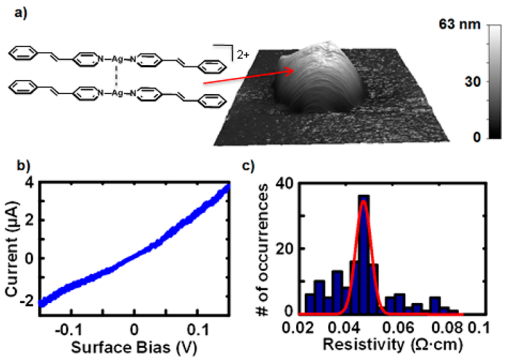

Figure 3. Complex **1**: (a) AFM height image, (b) *I*−*V* curve (height ~70 nm), and (c) distribution of resistivities (Gaussian fit red line).

Current−voltage (*I*−*V*) measurements were next collected on individual nanocrystals of **1** in air under 50 nN of force, which provided stable electrical contacts between each crystal and tip (Figure 3). Individual crystals were deposited on a Au substrate dropwise from hexane suspensions. Resistances for each nanocrystal (Figure 3a) were determined using the linear Ohmic region of the *I*−*V* curve within ±0.05 V (Figure 3b). The bias range was fitted using Ohm's law to determine resistance (*R*), and the resistivity (ρ) was then obtained using $\rho = Ra/l$, where *l* is crystal height and *a* is contact area between the probe and sample. Crystal heights were determined directly using AFM height images.[29] The contact area was determined using the hertzian elastic contact model.[33,37] The elastic

dx.doi.org/10.1021/ja4131774 | J. Am. Chem. Soc. 2014, 136, 6778−6781

modulus was directly measured using AFM nanoindentation (see SI, Figure S7). The Young's modulus of **1** was determined to be 505 ± 85 MPa, with the contact area at force of 50 nN as 1450 ± 150 nm^2.

A Gaussian fit to distribution of resistivities (Figure 3c) yielded a mean resistivity of (4.8 ± 0.3) × 10^{-2} Ω·cm for **1**, which corresponds to an electrical conductivity of (20.8 ± 1.3) S·cm^{-1}. The conductivity is outstanding for a metal−organic solid, being significantly higher than that of [Ag_2(ophen)$_2$].[7,38] We attribute the high conductivity to the face-to-face $\pi-\pi$ interactions of the stilbazoles, assisted by Ag···Ag forces.[39]

We next examined the effects of photodimerization on the conductivity.[40,41] Thus, the elastic modulus and electrical conductivity of photodimerized **2** were measured using CP-AFM (Figure 4). An AFM image revealed crystals of heights

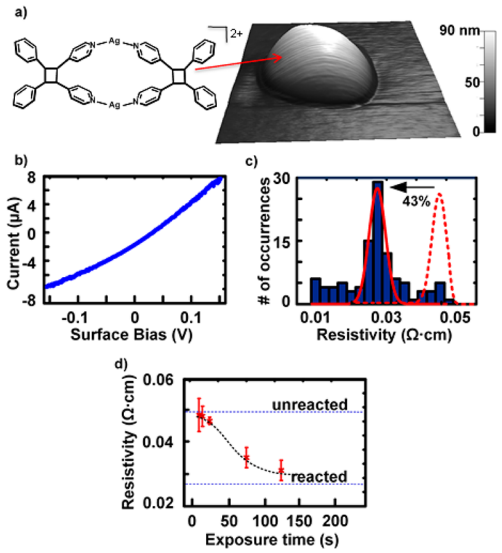

Figure 4. Complex **2**: (a) AFM height image, (b) *I*−*V* curve (height ~75 nm), (c) distribution of resistivities (Gaussian fit red line, dashed line response of **1**), and (d) *in situ* CP-AFM showing decrease in resistivity of **2** versus UV exposure (blue lines as averaged responses, black line as eye guide).

and morphologies similar to those of **1** (Figure 4a), while PXRD was consistent with crystallinity maintained after photodimerization (see SI, Figure S2). From AFM measurements, the Young's modulus was determined as 305 ± 50 MPa with a contact area at force of 50 nN as 2025 ± 200 nm^2,[42] which corresponds to a resistivity of (2.7 ± 0.3) × 10^{-2} Ω·cm and electrical conductivity of 37.0 ± 4.1 S·cm^{-1}. Hence, in the SCSC cycloaddition of **1** to **2**, the solid underwent an approximately 40% increase in conductivity.

The electrical response of an individual nanocrystal as a function of UV light exposure was also measured *in situ* using CP-AFM. The measurement revealed an average resistivity before photoreaction of (4.7 ± 0.3) × 10^{-2} Ω·cm. Exposures to UV light were performed from the side of the AFM tip, which allowed measurements in real time during the photodimerization. Four sequential UV exposures were applied, up to a total of 135 s, and after each exposure the nanocrystal was reimaged and resistivity was determined (Figure 4d). Whereas the crystal remained intact with no obvious changes in size or shape (see SI, Figure S10), a steady decrease in the resistivity up to 32% was observed, which is consistent with the averaged response (40%). The *in situ* experiment unambiguously supports the nanocrystals becoming more conductive after photoreaction.

The increase in conductivity can be attributed to a combination of effects. A quantum chemical analysis of the crystal data of **2** to calculate density of states (DOS) revealed the highest-occupied crystalline orbital (HOCO) energies to be located close to the work function of the Au substrate, while the lowest-unoccupied crystalline orbital (LUCO) levels are at significantly higher energies (see SI). Hence, the HOCO likely plays a dominant role in facilitating charge transport in the solid.[43] The calculations also reveal a 20% higher contribution of the Ag(I) ions at the top edge of the valence band of **2** compared to **1**. Contributions from the coordinated olefins also diminish upon photoreaction (see SI, Figure S11). Moreover, provided the conductivity proceeds via charge hopping,[44,45] the diffused orbital shell of the Ag(I) ions can be expected to have enhanced charge carrier mobility in the solid. The strained cyclobutane rings and Ag···C(phenyl) forces of the coordination polymer may also act as efficient electron donors.[46,47] We also note that there is no evidence of photoreduction of Ag(I) in the SCSC transformation. The crystals remain transparent during the photoreaction and PXRD shows no peaks from Ag (see SI, Figure S4). UV−vis spectroscopy also shows no characteristic absorption band for photoreduced Ag(I) particles (see SI, Figure S12).[48,49] The conductivity is, thus, intrinsic of the metal−organic solid.

Solid-state fluorescence of conductive materials is relevant to design solids as light emitting diodes and electronic displays.[18] In this context, the solid-state fluorescence of **1** revealed an emission band at 398 nm, attributable to 4-stilbz.[50] Photoreacted **2** displayed an emission band with two peaks at 360 and 396 nm (see SI, Figure S9).[51−53] The SCSC reaction was, thus, accompanied by a blue shift in fluorescence, in line with a loss of conjugation of 4-stilbz.[54]

To gain further insight into the change in conductivity, nanocrystals of isostructural **3** and **4** were generated.[23] The resistivity of **3** was determined to be 0.86 ± 0.47 Ω·cm, which corresponds to a conductivity of 1.17 ± 0.41 S·cm^{-1}. Moreover, the resistivity of photodimerized **4** was 0.67 ± 0.58 Ω·cm, which corresponds to a conductivity of 1.50 ± 0.84 S·cm^{-1}. Hence, as with **1** and **2**, a significant increase in electrical conductivity (~30%) was realized in the SCSC reaction of **3** to **4**. The increase in conductivity was also reflected in DOS calculations, which revealed a 15% higher contribution of the Ag(I) ions to the edge of the valence band of **4**.

In conclusion, we have described a dimetal Ag(I) complex that exhibits high electrical conductivity that increases in a SCSC [2+2] photodimerization. We are turning to apply principles of crystal engineering to electrical properties of additional metal−organic materials.

■ ASSOCIATED CONTENT

Supporting Information

Experimental details, single-crystal and powder XRD data, ^{1}H NMR, UV−vis, and fluorescence spectra, and DFT calculations. This material is available free of charge via the Internet at http://pubs.acs.org. Supplementary crystallographic data (CCDC 945407−945408) can be obtained free of charge from the Cambridge Crystallographic Data Centre via www.ccdc.cam.ac.uk/conts/retrieving.html.

dx.doi.org/10.1021/ja4131774 | J. Am. Chem. Soc. 2014, 136, 6778−6781

AUTHOR INFORMATION

Corresponding Authors

alexei-tivanski@uiowa.edu
len-macgillivray@uiowa.edu

Notes

The authors declare no competing financial interest.

ACKNOWLEDGMENTS

L.R.M. gratefully acknowledges partial financial support from the National Science Foundation (DMR-1104650).

REFERENCES

(1) Desiraju, G. R. *J. Chem. Sci.* **2010**, *122*, 667.
(2) Braga, D.; D'Addario, D.; Giaffreda, S. L.; Maini, L.; Polito, M.; Grepioni, F. *Top. Curr. Chem.* **2005**, *254*, 71.
(3) Barbour, L. J. *Chem. Commun.* **2006**, 1163.
(4) Haynes, D. A. *CrystEngComm* **2011**, *13*, 4793.
(5) Mei, J.; Diao, Y.; Appleton, A. L.; Fang, L.; Bao, Z. *J. Am. Chem. Soc.* **2013**, *135*, 6724.
(6) Xu, Z. *Coord. Chem. Rev.* **2006**, *250*, 2745.
(7) Zheng, S. L.; Zhang, J. P.; Wong, W. T.; Chen, X. M. *J. Am. Chem. Soc.* **2003**, *125*, 6882.
(8) Gao, J. H.; Xu, B. *Nano Today* **2009**, *4*, 281.
(9) An, B. K.; Gihm, S. H.; Chung, J. W.; Park, C. R.; Kwon, S. K.; Park, S. Y. *J. Am. Chem. Soc.* **2009**, *131*, 3950.
(10) Garcia-Frutos, E. M. *J. Mater. Chem. C* **2013**, *1*, 3633.
(11) Hermosa, C.; Alvarez, J. V.; Azani, M. R.; Gomez-Garcia, C. J.; Fritz, M.; Soler, J. M.; Gomez-Herrero, J.; Gomez-Navarro, C.; Zamora, F. *Nat. Commun.* **2013**, *4*, No. 1709.
(12) Schmitt, R. D.; Wing, R. M.; Maki, A. H. *J. Am. Chem. Soc.* **1969**, *91*, 4394.
(13) Yao, Y. S.; Shen, W. T.; Nohra, B.; Lescop, C.; Reau, R. *Chem.—Eur. J.* **2010**, *16*, 7143.
(14) Munakata, M.; Wu, L. P.; Kuroda-Sowa, T.; Maekawa, M.; Suenaga, Y.; Ning, G. L.; Kojima, T. *J. Am. Chem. Soc.* **1998**, *120*, 8610.
(15) Munakata, M.; Ning, G. L.; Suenaga, Y.; Kuroda-Sowa, T.; Maekawa, M.; Ohta, T. *Angew. Chem., Int. Ed.* **2000**, *39*, 4555.
(16) Khlobystov, A. N.; Blake, A. J.; Champness, N. R.; Lemenovskii, D. A.; Majouga, A. G.; Zyk, N. V.; Schroder, M. *Coord. Chem. Rev.* **2001**, *222*, 155.
(17) Narayan, T. C.; Miyakai, T.; Seki, S.; Dinca, M. *J. Am. Chem. Soc.* **2012**, *134*, 12932.
(18) Roy, S.; Mondal, S. P.; Ray, S. K.; Biradha, K. *Angew. Chem., Int. Ed.* **2012**, *51*, 12012.
(19) Willner, I.; Willner, B. *J. Mater. Chem.* **1998**, *8*, 2543.
(20) Li, F.; Zhuang, J. P.; Jiang, G. Y.; Tang, H. H.; Xia, A. D.; Jiang, L.; Song, Y. L.; Li, Y. L.; Zhu, D. B. *Chem. Mater.* **2008**, *20*, 1194.
(21) Lu, S. X.; Liu, Y.; Shao, N.; Panchapakesan, B. *Nanotechnology* **2007**, *18*, No. 065501.
(22) Kim, T.; Al-Muhanna, M. K.; Al-Suwaidan, S. D.; Al-Kaysi, R. O.; Bardeen, C. J. *Angew. Chem., Int. Ed.* **2013**, *52*, 7027.
(23) Chu, Q. L.; Swenson, D. C.; MacGillivray, L. R. *Angew. Chem., Int. Ed.* **2005**, *44*, 3569.
(24) Crystal data for **1**: monoclinic, space group $C2/c$, a = 22.794(3) Å, b = 12.830(1) Å, c = 18.208(2) Å, β = 94.293(5)°, V = 5310.1(2) Å^3, for Z = 8 and R = 0.0869 for $I > 2\sigma(I)$.
(25) Schmidt, G. M. J. *Pure Appl. Chem.* **1971**, *27*, 647.
(26) Ohba, S.; Hosomi, H.; Ito, Y. *J. Am. Chem. Soc.* **2001**, *123*, 6349.
(27) Harada, J.; Ogawa, K. *J. Am. Chem. Soc.* **2001**, *123*, 10884.
(28) Crystal data for **2**: monoclinic, space group $C2$, a = 21.768(4) Å, b = 13.498(3) Å, c = 17.570(4) Å, β = 98.24(3)°, V = 5109.2(2) Å^3, for Z = 4 and R = 0.1291 for $I > 2\sigma(I)$.
(29) Kapadia, P. P.; Ditzler, L. R.; Baltrusaitis, J.; Swenson, D. C.; Tivanski, A. V.; Pigge, F. C. *J. Am. Chem. Soc.* **2011**, *133*, 8490.
(30) Kelley, T. W.; Frisbie, C. D. *J. Vac. Sci. Technol. B* **2000**, *18*, 632.
(31) Palermo, V.; Liscio, A.; Palma, M.; Surin, M.; Lazzaroni, R.; Samori, P. *Chem. Commun.* **2007**, 3326.
(32) Reid, O. G.; Munechika, K.; Ginger, D. S. *Nano Lett.* **2008**, *8*, 1602.
(33) Karunatilaka, C.; Bučar, D.-K.; Ditzler, L. R.; Friščić, T.; Swenson, D. C.; MacGillivray, L. R.; Tivanski, A. V. *Angew. Chem., Int. Ed.* **2011**, *123*, 8801.
(34) Burda, C.; Chen, X. B.; Narayanan, R.; El-Sayed, M. A. *Chem. Rev.* **2005**, *105*, 1025.
(35) Sander, J. R. G.; Bučar, D.-K.; Henry, R. F.; Zhang, G. G. Z.; MacGillivray, L. R. *Angew. Chem., Int. Ed.* **2010**, *49*, 7284.
(36) Bučar, D.-K.; MacGillivray, L. R. *J. Am. Chem. Soc.* **2007**, *129*, 32.
(37) Ditzler, L. R.; Karunatilaka, C.; Donuru, V. R.; Liu, H. Y.; Tivanski, A. V. *J. Phys. Chem. C* **2010**, *114*, 4429.
(38) For a recent study on electrical properties of a porous metal–organic framework, see ref 17.
(39) Givaja, G.; Amo-Ochoa, P.; Gomez-Garcia, C. J.; Zamora, F. *Chem. Soc. Rev.* **2012**, *41*, 115.
(40) Abousekkina, M. M. *Thermochim. Acta* **1986**, *101*, 1.
(41) Kanungo, M.; Lu, H.; Malliaras, G. G.; Blanchet, G. B. *Science* **2009**, *323*, 234.
(42) The decease contrasts 2(5-cyanoresorcinol)·2(*trans*-1,2-bis(4-pyridyl)ethylene), where a 40% increase was determined.[33]
(43) Kim, B.; Choi, S. H.; Zhu, X. Y.; Frisbie, C. D. *J. Am. Chem. Soc.* **2011**, *133*, 19864.
(44) Wang, S.; Ha, M. J.; Manno, M.; Frisbie, C. D.; Leighton, C. *Nat. Commun.* **2012**, *3*, No. 1210.
(45) Luo, L. A.; Choi, S. H.; Frisbie, C. D. *Chem. Mater.* **2011**, *23*, 631.
(46) Elacqua, E.; Bučar, D.-K.; Skvortsova, Y.; Baltrusaitis, J.; Geng, M. L.; MacGillivray, L. R. *Org. Lett.* **2009**, *11*, 5106.
(47) Yamaguchi, S.; Tatemitsu, H.; Sakata, Y.; Enoki, T.; Misumi, S. *J. Chem. Soc., Chem. Commun.* **1982**, 1065.
(48) Corde, J.; Perruchas, S.; Vieille, L.; Galaup, J.-P.; Duluard, S.; Biver, C.; Boilot, J.-P.; Gacoin, T. *Nanotechnology* **2012**, *23*, No. 50.
(49) Liu, H. L.; Ye, Y. J.; Chen, J.; Lin, D. Y.; Jiang, Z.; Liu, Z. J.; Sun, B.; Yang, L. B.; Liu, J. H. *Chem.—Eur. J.* **2012**, *18*, 8037.
(50) Cariati, E.; Roberto, D.; Ugo, R.; Ford, P. C.; Galli, S.; Sironi, A. *Inorg. Chem.* **2005**, *44*, 4077.
(51) Shizuka, H.; Seki, I.; Morita, T.; Iizuka, T. *Bull. Chem. Soc. Jpn.* **1979**, *52*, 2074.
(52) Samsonova, L. G.; Kopylova, T. N.; Svetlichnaya, N. N.; Andrienko, O. S. *High Energy Chem.* **2002**, *36*, 276.
(53) Tamura, H.; Shinohara, Y.; Arai, T. *Chem. Lett.* **2011**, *40*, 129.
(54) Gayathri, K.; Saravanan, C.; Kannan, P. *J. Polym. Sci., Part A: Polym. Chem.* **2009**, *47*, 5208.